Rotating radiative-convective equilibrium simulated by a cloud-resolving model

Citation: Khairoutdinov, Marat, and Kerry Emanuel. "Rotating Radiative-Convective Equilibrium Simulated by a Cloud-Resolving Model." Journal of Advances in Modeling Earth Systems 5, no. 4 (December 2013): 816–825. © 2013 American Geophysical Union

As Published: http://dx.doi.org/10.1002/2013ms000253

Publisher: American Geophysical Union (AGU)

Persistent URL: http://hdl.handle.net/1721.1/97936

Version: Final published version: final published article, as it appeared in a journal, conference proceedings, or other formally published context

Rotating radiative-convective equilibrium simulated by a cloud-resolving model

Marat Khairoutdinov[1] and Kerry Emanuel[2]

Received 2 August 2013; revised 22 October 2013; accepted 31 October 2013; published 24 December 2013.

[1] The results of a series of cloud-resolving radiative-convective equilibrium (RCE) simulations are presented. The RCE simulations, used as an idealization for the mean tropical climate, are run for a wide range of prescribed sea-surface temperatures (SSTs), from 21°C to 36°C, representing the range of past, present, and, possibly, future mean tropical SSTs. The RCE with constant Coriolis parameter f is contrasted with nonrotating RCE. The Coriolis parameter is artificially increased from typical values in the Tropics by about one order of magnitude to allow multiple tropical cyclones (TCs) to coexist in a relatively small 2300×2300 km^2 domain with a 3 km horizontal grid spacing. Nonrotating RCE is also simulated, but using a substantially smaller, 384×384 km^2 domain. Rotating RCE, which we nickname "TC World," contains from 8 to 26 TCs with the average number of TCs monotonically decreasing with increasing SST. At the same time, the TCs' size, intensity, and per-TC precipitation rate tend to increase in response to increasing SST. For example, the average per-TC kinetic energy and precipitation rate tend to double for every 6°C SST increase. These results are consistent with scaling laws in which TC velocities and inner core diameters scale with the potential intensity and its ratio to the Coriolis parameter, respectively, while the separation between cyclone centers appears to scale with the deformation radius. It is also found that the outflow temperature of TC's, as defined as the height of the local maximum of the upper-troposphere cloud fraction, remains relatively invariant with SST. The cold-point tropopause height in TC World is found to be about 2 km higher than the corresponding height in nonrotating RCE.

Citation: Khairoutdinov, M. F., and K. A. Emanuel (2013), Rotating radiative-convective equilibrium simulated by a cloud-resolving model, *J. Adv. Model. Earth Syst.*, *5*, 816–825, doi:10.1002/2013MS000253.

1. Introduction

[2] Tropical convection has a tendency to self-organize or aggregate on a wide range of scales that are generally much larger than the size of individual convective cells. When a few convective cells merge, they may form a cluster on the order of 10 km in size, such as an air-mass shower. When sufficient low-level vertical wind shear is present, a squall line may form. Under special circumstances, large mesoscale clusters of convection can develop, such as mesoscale convective complexes (MCC), tropical depressions, and tropical cyclones. Coupling of convection to equatorially trapped waves, such as Kelvin and equatorially trapped Rossby waves, can aid in the development of super-clusters. The ultimate tropical super-cluster of planetary scale is the Madden-Julian Oscillation (MJO), which, on closer inspection, is an envelope of clusters of different sizes moving in different directions with different propagation speeds. The mechanisms for aggregation of convection can be quite different for different types and scales of convective systems. Some mechanisms are better understood than others, but there is generally a poor understanding of how aggregated tropical convection will respond to global warming.

[3] Tropical convection has long been viewed as a process that stabilizes the atmosphere at the same rate that radiation and other large-scale processes destabilize it. This quasi-equilibrium postulate was first advanced by *Arakawa and Schubert* [1974]. On average, the Tropics absorb about 20% more solar energy than they emit as infrared radiation to space. The excess energy is exported to higher latitudes. Thus, to a large extent, on long spatial and time scales, the tropical atmosphere is not far from a state of radiative-convective equilibrium (RCE). In RCE, which is the simplest subset of quasi-equilibrium, the effects of the large-scale circulations are ignored, and the convection

[1]School of Marine and Atmospheric Sciences, Stony Brook University, Stony Brook, New York, USA.
[2]Department of Earth, Atmospheric, and Planetary Sciences, Massachusetts Institute of Technology, Cambridge, Massachusetts, USA

Corresponding author: M. Khairoutdinov, SoMAS, Stony Brook University, Stony Brook, NY 11794-5000, USA. (marat.khairoutdinov@stonybrook.edu)

1942-2466/13/10.1002/2013MS000253

reacts to destabilization only by the radiative cooling and surface enthalpy fluxes, computed assuming that the surface is an ocean with a calculated or prescribed sea-surface temperature (SST). The RCE model as an idealization of the tropical atmosphere has been used in one-dimensional numerical studies with parameterized convection [e.g., *Renno´ et al*., 1994]; in such models, no effects of convective organization on the atmospheric state have been included. Over the past decades, cloud-resolving models (CRMs) have become a standard tool for explicitly simulating clouds and cloud-systems over domains large enough to contain not only individual clouds but also organized convective systems. CRMs have also been used quite extensively to study problems related to the RCE idealization of the tropics [e.g., *Held et al*., 1993; *Islam et al*., 1993; *Robe and Emanuel*, 1996; *Tompkins and Craig*, 1998; *Xu and Randall*, 1999; *Tao et al*., 1999; *Grabowski*, 2006; *Romps*, 2011].

[4] As computer power increased, the size of numerical domains also grew, and eventually the aggregation of individual convective elements into large-scale clusters could be explicitly simulated. It has been shown that tropical convection in idealized RCE can be in either of two stable states: disorganized random convection and aggregated convection [*Bretherton et al*., 2005]. Unorganized convection generally results when domains of relatively small size, on the order of a hundred kilometers square, are used. However, with larger domains, the deep convection, under certain conditions, *spontaneously* aggregates into large "blobs" or clumps [*Bretherton et al*., 2005]. It has been found that the transition from random unorganized convection to clumps is a function of temperature; specifically, the convection remains random below a certain SST threshold even when a sufficiently large domain is used, and aggregates into clumps above that threshold [*Khairoutdinov and Emanuel*, 2010; *Wing and Emanuel*, 2012]. It has also been shown that aggregation is sensitive to the domain size [*Bretherton et al*., 2005] and even to the grid spacing used in the CRM [*Muller and Held*, 2012]. Another curious feature of aggregated convection in RCE is the apparent hysteresis of the transition to the convective clump. For example, once convection becomes aggregated above a certain SST threshold, it will remain aggregated even if the SST is reduced well below the threshold [*Khairoutdinov and Emanuel*, 2010; *Muller and Held*, 2012].

[5] *Bretherton et al*. [2005] and *Nolan et al*. [2007] found, using cloud-resolving models, that when phrased on an *f*-plane, convection in RCE spontaneously aggregates into a single tropical cyclone. The small domain size used in these studies likely prevented more than one cyclone from developing. The behavior of multiple coexisting tropical cyclone-like disturbances in an *f*-plane RCE run at GCM resolution with parameterized convection was studied by *Held and Zhao* [2008] (hereafter HZ08), who reported that the number of cyclone-like vortices tends to decrease with increasing SST, while their intensity increased. They also found that the number of the vortices decreases when the ambient rotation decreases.

[6] In this paper, we present the results of cloud-resolving *f*-plane RCE simulations with multiple coexisting tropical cyclones, a framework that we nickname "TC World." We explore the sensitivity of various statistics of the TC-World to SST prescribed over a rather wide range. The *f*-plain RCE simulations are complemented with a traditional RCE simulation with no planetary rotation. By comparing the statistics of these two frameworks and comparing their equilibrium climate sensitivities, we hope to advance the understanding of the role that TCs may play in the tropical climate system in current and future climates.

[7] The paper is organized as follows: section 2 describes the model and experimental setup, section 3 presents the results, and section 4 provides a summary.

2. Model Description and Setup

2.1. Model Description

[8] For all simulations, we use the System for Atmospheric Modeling (SAM) [*Khairoutdinov and Randall*, 2003], version 6.9. The model solves the system of nonhydrostatic momentum equations using an anelastic approximation. The subgrid-scale fluxes are parameterized using an eddy-conductivity/diffusivity model with Smagorinsky-Lilly first-order closure for the eddy coefficients [*Lilly*, 1962]. Surface fluxes are computed using the ocean-fluxes scheme adopted from the Community Atmosphere Model, version 3 (CAM3) [*Collins et al*., 2006]. The interactive radiation scheme is also adopted from CAM3. Liquid/ice static energy is assumed to be conserved in all moist adiabatic processes except for liquid/ice water sedimentation. Cloud microphysics are represented by a single-moment bulk scheme with two prognostic variables: the sum of nonprecipitating liquid/ice cloud water and water-vapor mixing ratios, and the total precipitation mixing ratio [*Khairoutdinov and Randall*, 2003]. The total cloud liquid/ice content is diagnosed from the prognostic variables using the so-called "all-or-nothing" condensation/sublimation scheme. The partition of the cloud water into liquid and ice phases as well as of precipitating water into rain, snow, and graupel is assumed to be a predefined function of temperature only. During the microphysics stage of computations, the warm and cold microphysical conversion rates as well as sedimentation velocities are computed for each of the diagnosed hydrometeors, which are then combined into their respectful prognostic variables. The use of only two prognostic water variables saves considerable computer time as each prognostic thermodynamic variables is transported using a monotonic and sign-preserving advection algorithm of *Smolarkiewicz and Grabowski* [1990].

2.2. TC-Size Scaling

[9] In order to minimize the effect of the domain size on the statistics of the *f*-plane RCE, the domain should be large enough to contain several tropical cyclones at all times. We conducted an experiment using a doubly periodic 3000×3000 km^2 domain with a Coriolis parameter corresponding to 20^o latitude. The initial

state of the atmosphere was horizontally uniform with convection initiated by random small-amplitude temperature noise near the surface, with a prescribed SST of 300 K. A single TC spontaneously developed, as shown in Figure 1a. One can see that the domain size was barely sufficient to contain the single TC. In order to fit several TCs of that size, we would need a domain several times as large as the one used in the experiment. It would not be computationally feasible to perform even a single RCE simulation using such a large domain, as it usually requires several weeks of simulation time to reach equilibrium.

[10] To manage computational cost, one could make the cyclones smaller instead of making the domain larger. *Emanuel* [1986] showed that TC sizes are bounded above by

$$D = \frac{V_p}{f} \tag{1}$$

where V_p is the potential intensity. The noncloud-resolving simulations of HZ08 and also the recent work of *Chavas* [2013] suggests that this scale also governs the size of TCs in RCE states. It is not straightforward to change the PI considerably and still have an Earth-like basic state; however, it is easy to change the Coriolis parameter. We repeated the experiment described above, but this time with the Coriolis parameter ramped up by a factor of 4. As a result, as many as five TCs developed with sizes that generally follow the scaling (1) reasonably well, as illustrated in Figure 1b.

2.3. Case Setup

[11] Based on the results of the TC-size scaling test, we set f at the even higher value of 5×10^{-4} s^{-1}, which would result in many TCs coexisting in a 2300 × 2300 km^2 domain. Although the individual TCs are much smaller than observed, they are still far larger than individual clouds. To examine the effect of the TCs on RCE statistics, each f-plane RCE run is complemented with a nonrotating RCE run over a smaller 384 × 384 km^2 domain. All simulations use a doubly periodic horizontal domain with a horizontal grid spacing of 3 km. In each simulation, the SST is fixed; the values span a rather wide range: 21, 24, 27, 30, 33, and 36°C. Note that over the present Tropics (30°S–30°N), the SSTs under the regions of deep convection, where TCs form, are generally in the 27–30°C range.

[12] The vertical grid stretches gradually from the smallest grid spacing of 50 m near the surface to 150 m at 1 km, and finally to 500 m above 5 km. To minimize the reflection of gravity waves from the top of the domain, Newtonian damping is applied in the upper 30% of the domain, with damping strength gradually increasing upward. To minimize the effect of damping on convection in the troposphere, which becomes generally deeper with warmer SSTs, the domain height is 28 km for SSTs cooler than 33°C and 33 km for SSTs warmer than 33°C. The incoming solar radiation is set to a perpetual insolation of 400 W/m^2, which roughly corresponds to the daily-mean insolation over the main TC-active regions in the Tropics during active periods. To avoid long initial spin-up time, the initial soundings for each SST have been generated by separate 100 day long RCE runs that use a much smaller 96 × 96 km^2 domain. Following classical RCE methodology, there is no prescribed large-scale dynamical forcing and no mean wind. All simulations are initialized by small-amplitude random noise in the temperature field in the few lowest layers of the grid. Surface fluxes are

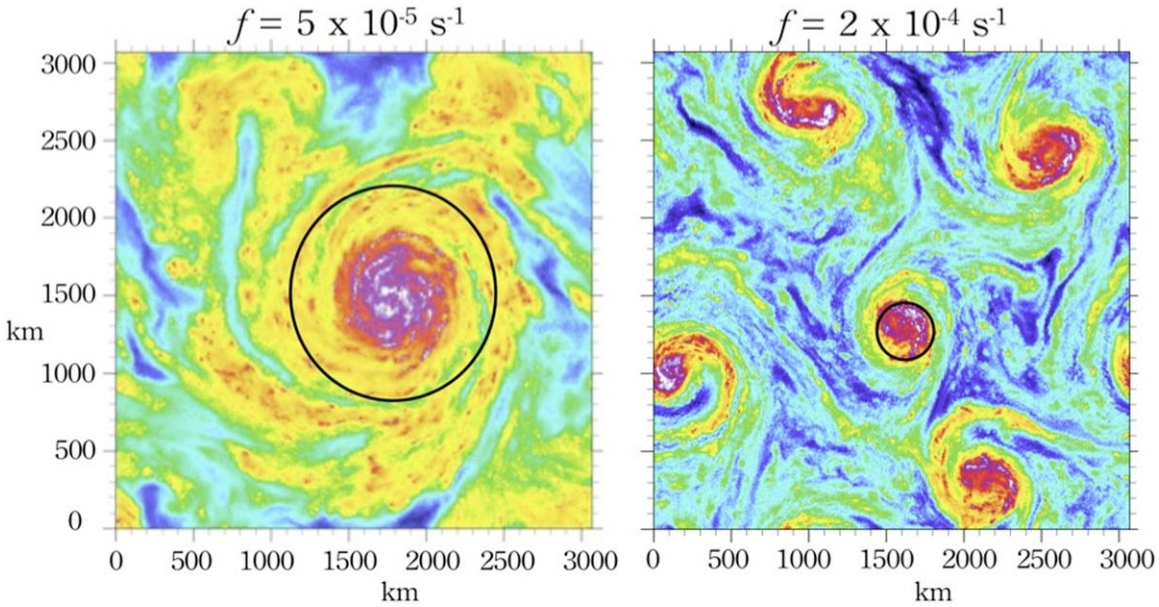

Figure 1. Tropical cyclones for two different values of the Coriolis parameter in otherwise identical RCE simulations (precipitable water is shown; warm colors represent higher values). The black circles on the foreground have diameters computed from formula (1).

computed using the ocean-flux parameterization from the CAM3 model, and they are allowed to vary horizontally depending on the atmospheric conditions above. The time step is 12 s. All simulations are 100 days long.

3. Results

[13] It takes at least 2 months of simulation time to spin-up TCs and reach RCE over the given SST. During the final 40 day period of each run, the statistics are quite stationary; therefore, that period has been used for the statistical sampling.

3.1. The Effect of Warming SSTs on TC Frequency, Size, and Intensity

[14] Table 1 lists several key statistical measures of the TC-World as a function of SST, including the mean number of TCs. Although SST is a convenient control variable for our simulations, it should not be regarded as a fundamental control variable for tropical cyclones, whose properties in three dimensions depend largely on potential intensity and the Coriolis parameter [*Chavas*, 2013]. Even though we choose an SST range that spans those estimated to have occurred in the Tropics at various times in Earth's history, one should use caution in interpreting these results, especially given that surface energy balance is not maintained, owing to the specification of SST. Thus, we should interpret our results as functions of potential intensity rather than SST.

[15] Typical snapshots of the surface pressure field for each of the SSTs are shown in Figure 2. One can see that, in general, as SST increases, the size of the TCs tends also to increase, while their number tends to decrease. These results are qualitatively consistent with the noncloud-resolving results of HZ08. Figure 3 shows probability distribution functions (PDFs) of several TC bulk characteristics as a function of SST. TC size (Figure 3a), defined as the mean diameter of the 990 mb surface pressure isobar, shows a factor of 3–4 difference between the largest and smallest TC for each SST category. There is also a tendency for the TCs to deepen more in the warmer climate, as shown by the PDF of the minimum surface pressure (Figure 3b). A rough estimate for the increase of pressure minimum for a 1-K SST increase is 3–4 mb K^{-1}, which is consistent with the estimates made at GCM resolutions [*Knutson et al.*, 1998 (HZ08)]. The near-surface maximum wind speed as a measure of TC intensity also tends to increase with SST (Figure 3c), generally following the increase of potential intensity (Table 1). This is also consistent with HZ08. The average kinetic energy (KE) per unit area closely follows the trend of V_p, roughly at the rate of 1–2% per 1°C of SST increase. When normalized by the average number of the TCs, the KE-per-TC increases rather dramatically with SST (see Table 1), roughly doubling every 6°C of SST increase. As the KE is mostly localized within the TCs themselves, the tendency of the KE-per-TC can be viewed as an estimate of the tendency of the total KE associated with a single TC. As the precipitation in TC-World is also mostly localized within the TCs, the mean surface precipitation normalized by the total number of cyclones (Table 1) can also be viewed as proportional to the total precipitation associated with a single TC. One can see that this measure of latent heat release in a single TC also closely follows the trend of roughly doubling every 6°C of SST warming.

[16] These results show that TCs become larger and more powerful but less numerous, as SST increases. As expected, the domain integrated kinetic energy scales very nearly as V_p^2. On the other hand, if the interstorm scale is V_p/f, then the number of TCs in the domain should scale as f^2/V_p^2, but in fact the number decreases far more rapidly than this. We hypothesize that while the storm dimensions may indeed follow V_p/f scaling as in *Chavas* [2013], the distance between storm centers may scale more like a deformation radius. In a moist adiabatic atmosphere, the deformation radius scales with $\sqrt{e^*}/f$, where e^* is a representative saturation vapor pressure, which we take to be that associated with the SST. More details are given in Appendix. This hypothesis, therefore, predicts that the number of TCs in the domain should scale as f^2/e^*. Regressing $1/e^*$ based on SST against the number of TCs listed in Table 1 yields an r^2 of 0.97, an excellent fit (see Figure A2 in Appendix). This is also consistent with Figure 2, which seems to show that the proportion of "dead space" between TCs increases with SST. The evidence

Table 1. TC-World Simulation Statistics[a]

SST (°C)	21	24	27	30	33	36
N_{TC}	26	22	15	14	12	8
V_p (m/s)	52.6	55.7	58.6	61.5	62.6	63.8
KE (J/m^2)	0.34	0.38	0.43	0.45	0.46	0.49
KE/N_{TC} (J/m^2)	0.014	0.017	0.029	0.032	0.038	0.061
PR/N_{TC} (mm/day)	0.12	0.15	0.25	0.30	0.38	0.60
LW_{TOA} (W/m^2)	257.2	263.9	267.8	271.2	275.1	278.6
LW_{SFC} (W/m^2)	73.1	64.0	52.8	43.3	33.7	25.0
SW_{TOA} (W/m^2)	370.9	370.7	368.7	370.7	374.4	376.0
SW_{SFC} (W/m^2)	279.5	273.5	266.4	262.9	261.1	259.2

[a]Here N_{TC} is the average number of tropical cyclones; V_p is the TC's potential intensity; KE is the average kinetic energy per unit area; KE/N_{TC} is the average kinetic energy per unit area per TC; PR/N_{TC} is the precipitation rate per unit area per TC; and net longwave (LW) and shortwave (SW) fluxes at the top-of-atmosphere (TOA) and surface (SFC).

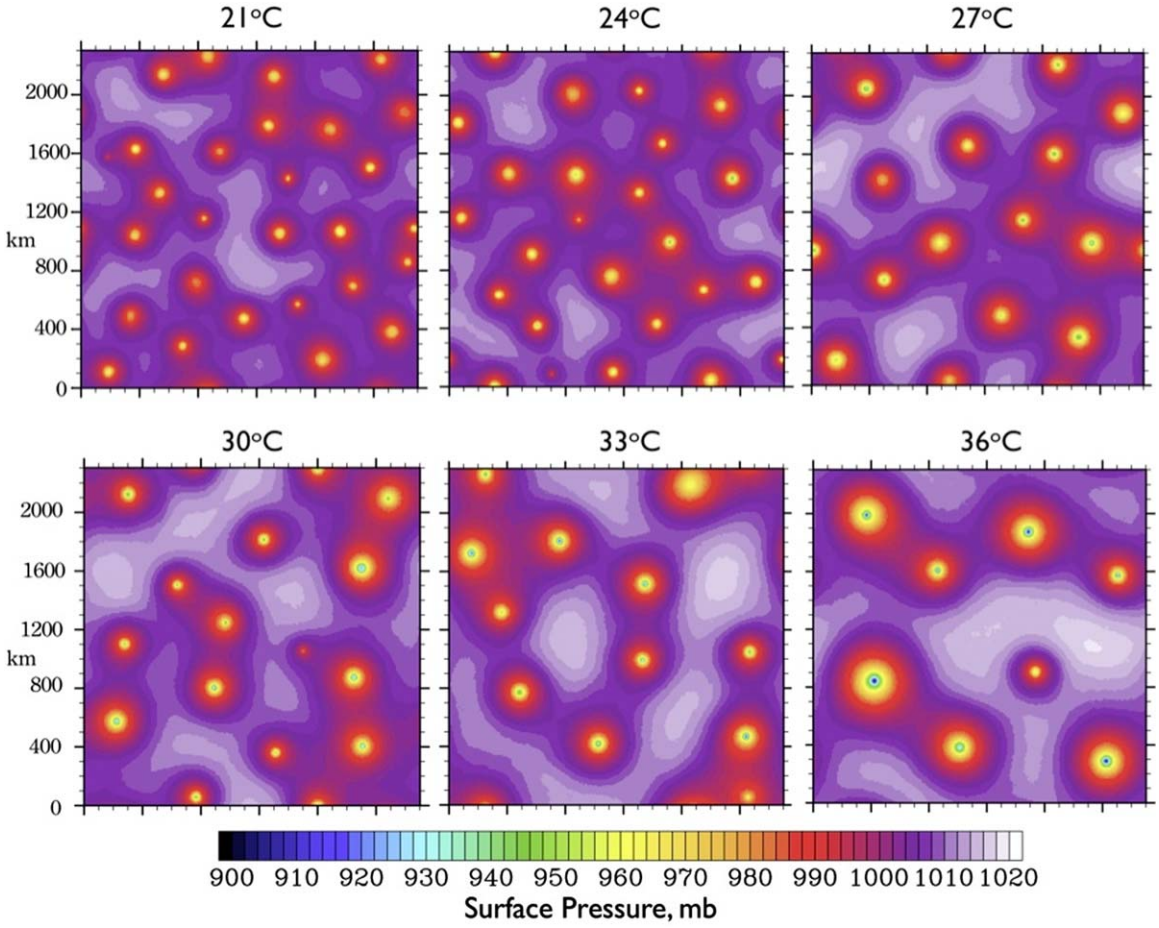

Figure 2. Snapshots of the surface pressure from the *f*-plane RCE simulations for different values of the SST.

presented here thus suggests that while the individual storm dimensions scale with V_p/f, the interstorm spacing scales as $\sqrt{e^*}/f$. It is also shown in Appendix that V_p scales with the cube root of the net radiative cooling of the troposphere.

[17] While these results are broadly consistent with predictions of the response of TCs to global warming [e.g., *Knutson et al.*, 2010], the conditions of our experiments are too far from those of the actual atmosphere to draw specific connections.

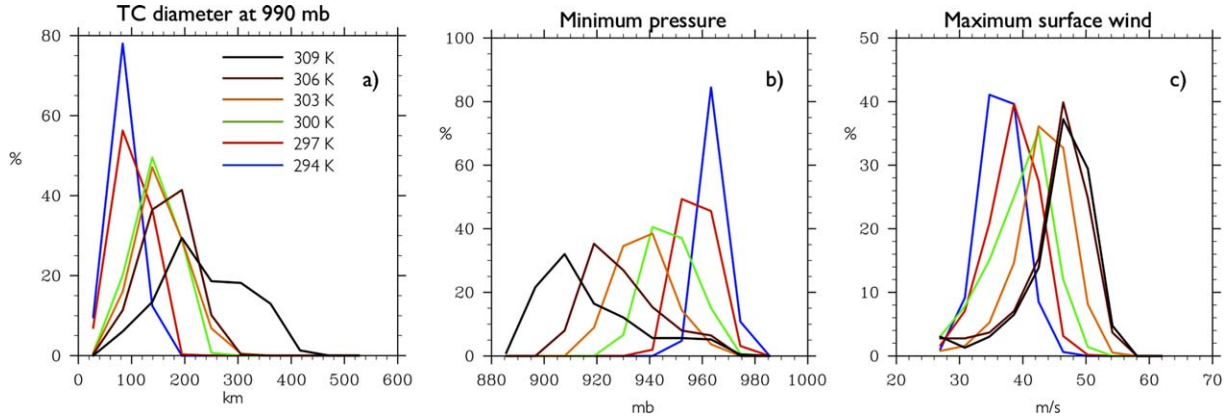

Figure 3. PDFs of TC (a) diameter at 990 mb, (b) minimum surface pressure, and (c) maximum surface wind in TC World.

3.2. The Effect of Warming SSTs on TC Outflow Temperature

[18] The response of the mean temperature profile to increasing SST is shown in Figure 4a. One can see that the cold-point tropopause rises with SST. A similar response of the tropopause is simulated in the nonrotating cases (not shown); however, the height of the tropopause in the TC-World simulations is considerably higher, by about 2 km. The temperature profile above the tropopause, in the simulated stratosphere, is relatively invariant with SST. This is most likely because the simulated stratosphere, with no large-scale transport, is close to a state of radiative equilibrium set mostly by the prescribed constant ozone profile. It is apparent that the temperature profile is steepening with the rise of SST, as dictated by the steepening moist-adiabatic lapse rate for warmer tropospheric temperatures. As a result, the upper-tropospheric temperature tends to increase more than the underlying SST.

[19] One may expect that the TCs' outflow temperature would closely follow the upper-tropospheric temperature. But this is generally not the case in our simulations if we define the outflow level as the level of maximum cloud fraction. Figure 4b shows the vertical profile of the cloud fraction in the TC-World using mean tropospheric temperature as the vertical coordinate. One can see that the outflow temperature in the TC-World is approximately constant and invariant with SST. This result is consistent with the Fixed Anvil Temperature (FAT) hypothesis proposed by *Hartmann and Larson* [2002] for tropical deep convection. The plausibility of the FAT hypothesis was demonstrated by *Kuang and Hartmann* [2007], who simulated nonrotating RCE over prescribed SST in the range of 26.5–

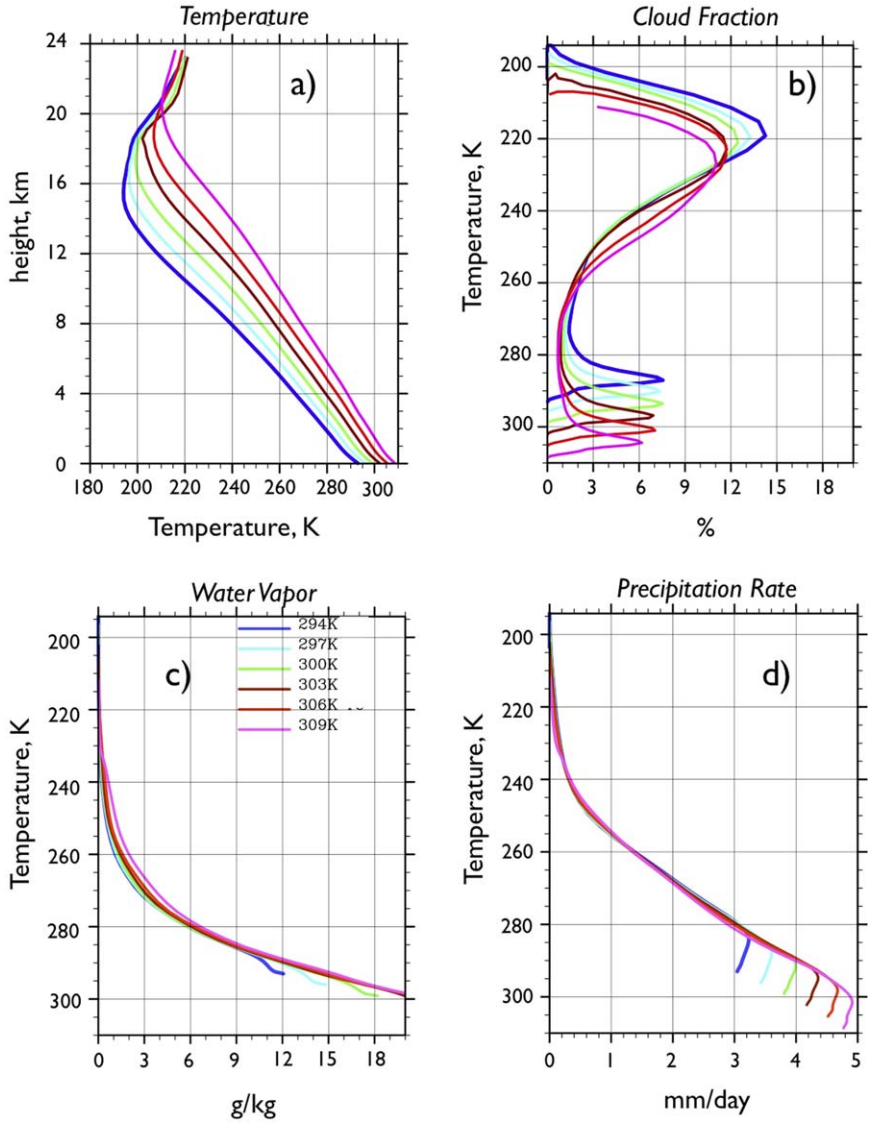

Figure 4. Vertical profiles of (a) temperature, (b) cloud fraction, (c) water vapor mixing ratio, and (d) precipitation rate for different SSTs. Note that in Figures 4b–4d temperature is used as the vertical coordinate rather than height. The color code for the six different SSTs is given in Figure 4c.

32.5°C using one of the earlier versions of the SAM model. Note that the FAT seems to hold in the nonrotating RCE simulations (not shown).

[20] One interesting aspect of our RCE simulations is the apparent similarity of several thermodynamic profiles above the boundary layer as they merge into a single curve when plotted using tropospheric temperature as the vertical coordinate. Figures 4b and 4c demonstrate such behavior for the profiles of water vapor and precipitation rate, respectively, in the TC-World. Similar behavior is found in the nonrotating RCE simulations. This behavior is consistent with the theoretical response to global warming discussed by *Singh and O'Gorman* [2012].

3.3. Hydrological Cycle and Number of Tropical Cyclones

[21] It is well known that the strength of the hydrological cycle, quantified by the precipitation rate averaged over large spatial and temporal scales, such as the whole Tropics, does not scale with the abundance of the atmospheric water vapor according to the Clausius-Clapayron (CC) relation [e.g., *Betts*, 1998; *Held and Soden*, 2006]. This notion is illustrated by Figure 5, which shows the dependence of the surface precipitation (Figure 5a) and column-integrated water vapor or precipitable water (Figure 5b) on SST. One can see that while the precipitable water increases by a factor of 3–4 in response to SST increase over the 15°C range, the precipitation increases at much slower rate, by a factor of 1.5–2.0. For the present-climate range of SSTs, the increase of precipitation is about 4%/°C for the norotating RCE versus about 3%/°C for the TC-World case. The corresponding rates for the precipitable water are 10%/°C and 9.5%/°C, respectively.

[22] Energy balance of the atmosphere dictates that the surface enthalpy flux (which at these SSTs is comprised mostly of the latent heat flux) balances the divergence of the net radiative flux across the whole atmospheric column. The latter does not scale with the CC relation. The surface evaporation (latent heat flux) must in turn balance precipitation, which scales as the product of the water vapor mixing ratio in the boundary layer and the convective mass flux. As the surface evaporation, and therefore the precipitation, increases at a much slower rate than the water vapor in the boundary layer, it follows that the convective mass flux associated with precipitating deep convection should decrease with SST. This is illustrated by Figure 5c, which shows a monotonic decrease of the local maximum of the mass flux above 3 km as SST increases. We chose 3 km height to avoid counting the mass flux associated with the shallow convection. As the shallow clouds produce relatively insignificant precipitation compared to deep clouds, the above CC-scaling argument does not apply to them.

[23] The reduction of the mass-flux associated with precipitating deep convection in response to SST warming is generally consistent with the reduction of the total number of the TCs with increasing SSTs in our TC-World simulations. As the cyclones in the TC-World become larger and more intense with warming SSTs, they have larger convective mass-flux associated with each cyclone, which is supported by about a 50% increase of the maximum updraft velocity in the TC-World for the prescribed increase of SSTs (not shown). Thus, the total number of the tropical cyclones in the TC-World should decrease with increasing SST, which is consistent with our results.

4. Summary

[24] In this study, we present the results of a series of cloud-resolving simulations of radiative-convective equilibrium (RCE) using a wide range of prescribed SSTs, in 3°C increments, from 21°C to 36°C. The novel aspect of this RCE study is the use of an artificially large Coriolis parameter to simulate the statistics and climate sensitivity of RCE containing multiple coexisting tropical cyclones (TCs). Coexistence of multiple TCs in the domain mitigates the concern that the domain size may affect the results. The *f*-plane RCE, nicknamed "TC World," was complemented with more traditional RCE with no planetary rotation. Contrasting the TC-World to nonrotating

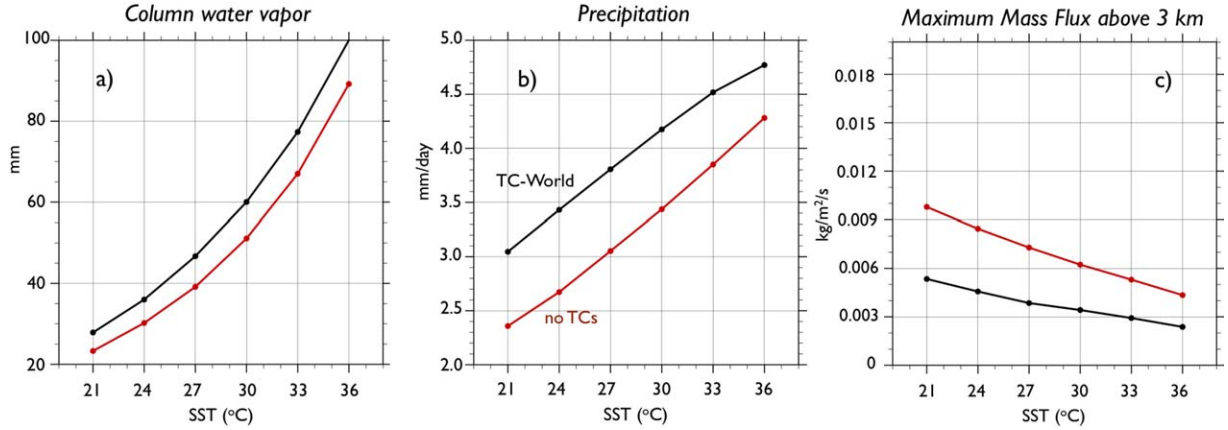

Figure 5. Sensitivity of (a) column integrated water vapor or precipitable water, (b) surface precipitation rate, and (c) mass flux maximum above 3 km in no-rotating (red) and *f*-plane "TC-World" (black) RCE simulations.

RCE in response to SST change as a proxy for climate change can help us better understand the role that TCs play in the present Tropics, as well as their possible role in a warmer future.

[25] To manage the high-computational cost required to simulate the TC World with multiple coexisting TCs, the Coriolis parameter f was substantially increased, by about an order of magnitude, from its typical values in the Tropics. This reduces the TC's characteristic size, which, as shown by other studies, is inversely proportional to f. As a result, in our simulations, the 2300×2300 km^2 domain contains anywhere from 8 to 26 TCs, depending on SST. To contrast the TC-World results to the nonrotating RCE, a substantially smaller domain, 384×384 km^2, was also used. All simulations were conducted with relatively course 3 km grid spacing. The vertical domain had its top as high as 33 km to minimize the effect of gravity-wave damping in the stratosphere. All the simulations were performed with interactive shortwave and longwave radiation, and also interactive surface latent and sensible fluxes. Each case was run for 100 days, with the last 40 days used for statistics sampling.

[26] The main findings of this idealized study are:

[27] 1. The average number of TCs monotonically decreases with increasing SST, following an f^2/e^* scaling, where e^* is the saturation vapor pressure associated with the SST.

[28] 2. The potential intensity V_p scales with the cube root of the net radiative cooling of the troposphere.

[29] 3. The size and intensity of TCs monotonically increase in response to increasing SST, with intensity scaling with potential intensity and inner core size scaling with V_p/f. The average kinetic energy per TC roughly doubles for every 6°C of SST increase.

[30] 4. The minimum surface pressure in the simulated TCs monotonically decreases with rising SST.

[31] 5. The precipitation per TC roughly doubles every 6°C of SST increase.

[32] 6. The cold-point tropopause height in TC World is about 2 km higher than its height in the nonrotating RCE.

[33] 7. The outflow temperature of TCs stays approximately constant.

[34] 8. The reduction of the number of the TCs in the TC-World with increasing SST is consistent with the monotonic decrease of the net mass flux carried mostly by the TCs, because of the inability of precipitation generated by the TCs to scale with the rapidly increasing amount of water vapor following the Clausius-Clapayron relation.

Appendix A: TC-World Scaling

[35] We first assume that most of the upward mass flux in TC-World occurs in the cores of tropical cyclones. The upward mass flux per unit area can be obtained from Ekman balance in the TC boundary layer, which shows that the upward velocity in steady-state TCs scales as $C_D V_p$, where C_D is the drag coefficient and V_p is the potential intensity, which we assume is the characteristic azimuthal velocity scale for TCs. Per TC, then, the area integrated TC mass flux scales as $C_D V_p r_m^2$, where r_m is the radius of maximum winds, which we assume is the correct scale for the radius at which the vertical velocity changes sign. Thus, the mass flux per unit area M scales as

$$M \sim C_D V_p \frac{r_m^2}{D^2} \tag{A1}$$

where D is a characteristic distance separating TC centers. In RCE, the heating owing to TC updrafts balances the vertically integrated radiative cooling $\dot{Q}$:

$$C_D V_p \frac{r_m^2}{D^2} c_p \overline{T} \Delta \ln(\theta) \approx \dot{Q} = F_{\mathrm{TOA}} - F_s \tag{A2}$$

where c_p is the heat capacity of air at constant pressure, $\Delta \ln(\theta)$ is the change in the logarithm of the potential temperature across the depth of the troposphere, $\overline{T}$ is the $\ln(\theta)$-weighted mean temperature of the troposphere, F_{TOA} is the net upward radiative flux at the top of the atmosphere (TOA), and F_s is the net upward radiative flux at the surface.

[36] Assuming that the troposphere has a moist adiabatic temperature lapse rate, then $c_p \overline{T} \Delta \ln(\theta) \approx -L_v \Delta q^* \approx L_v q_b$, where L_v is the latent heat of vaporization, Δq^* is the change in saturation specific humidity across the moist convecting layer, and we assume that this scales as the boundary layer specific humidity, q_b. With this substitution, equation (A2) becomes

$$C_D V_p \frac{r_m^2}{D^2} L_v q_b \approx F_{\mathrm{TOA}} - F_s \tag{A3}$$

[37] We put this heat balance relationship aside for the moment and focus on the domain-averaged energy balance. We assume that in TC-World, the entropy production is dominated by frictional dissipation of wind energy in the boundary layer. Then, the energy balance per unit area scales as

$$C_D V_p^3 \frac{r_o^2}{D^2} \sim \varepsilon \dot{Q} = \varepsilon (F_{\mathrm{TOA}} - F_s) \tag{A4}$$

where r_o is a characteristic radial scale over which dissipation occurs, and

$$\varepsilon = \frac{T_s - T_o}{T_o} \tag{A5}$$

where T_s is the surface temperature and T_o is the inverse of the mean inverse temperature at which radiative cooling occurs in the system. The right side of equation (A4) represents the export of entropy to space, while the left side is the creation of entropy by frictional dissipation in TCs.

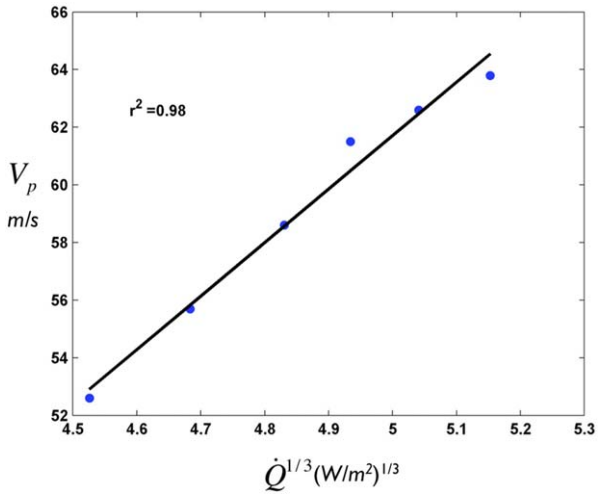

Figure A1. Potential intensity V_p regressed with the cube root of the net radiative cooling of the atmosphere Q.

[38] The ratio of equation (A4) to equation (A3) gives

$$V_p^2 \frac{r_o^2}{r_m^2} \approx \varepsilon L_v q_b \tag{A6}$$

[39] From the work of *Chavas* [2013], we assume that

$$r_m \approx \alpha \frac{V_p}{f} \tag{A7}$$

where f is the Coriolis parameter and α is a constant that is much smaller than 1. Substituting equation (A7) into equation (A6) gives

$$r_o^2 \approx \varepsilon \alpha^2 \frac{L_v q_b}{f^2} \tag{A8}$$

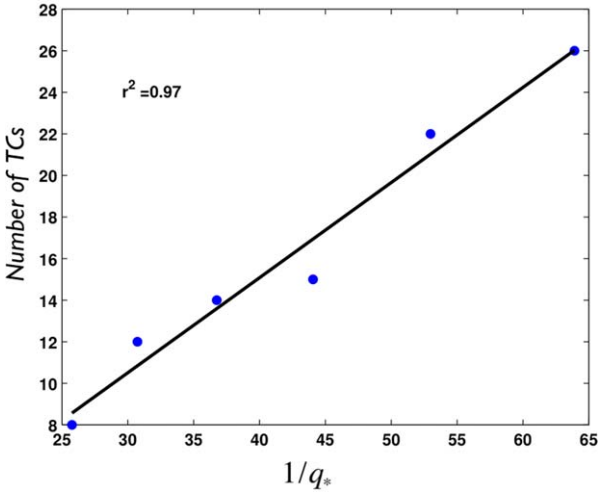

Figure A2. Number of TCs in domain regressed with the inverse saturation specific humidity at the SST.

[40] Thus, we predict that the characteristic scale at which dissipation occurs scales with $\sqrt{q_b}/f$, which can be shown to be proportional to the deformation radius in a moist adiabatic atmosphere. We make one more assumption: we assume that the characteristic separation distance between TCs, D, varies as $D = r_o/\gamma$ where γ is a constant such that $0 < \gamma < 1$. Using this in equations (A8) and (A4) gives

$$V_p^3 \approx \frac{\varepsilon(F_{TOA} - F_s)}{C_D \gamma^2} \tag{A9}$$

[41] Thus, we predict that the potential (and therefore actual) peak wind speed in the TCs scales with the cube root of the net radiative cooling of the troposphere. (Note that equation (A9) is independent of α). As shown in Figure A1, our TC-World results are consistent with the relationship (A9).

[42] Finally, we note that the number of TCs, n, in a box of dimension $L \times L$ varies as

$$n \sim \frac{L^2}{D^2} = \frac{\gamma^2}{\varepsilon \alpha^2} \frac{L^2 f^2}{L_v q_b} \tag{A10}$$

[43] Thus, we predict that in a domain of a fixed size, the number of TCs increases with the square of the Coriolis parameter but decreases with the boundary layer specific humidity. The latter closely follows the saturation specific humidity, which, of course, increases rapidly with increasing SST. This scaling is consistent with our TC World results shown in Figure A2.

[44] **Acknowledgments.** Kerry Emanuel was supported by the NSF grant AGS1032244 to MIT. Marat Khairoutdinov was supported by the NSF grant AGS1032241 to Stony Brook University, and also by the NSF Science and Technology Center for Multiscale Modeling of Atmospheric Processes (CMMAP), managed by Colorado State University under cooperative agreement ATM-0425247. The authors would like to thank the Indian Institute for Tropical Meteorology (IITM) in Pune, India, and especially its director, B. N. Goswami, for providing access to the supercomputer "Prithvi" where all the model integrations for this study have been performed.

References

Arakawa, A., and W. H. Schubert (1974), Interaction of a cumulus cloud ensemble with the large-scale environment, Part I, *J. Atmos. Sci.*, *31*, 674–701.

Betts, A. K. (1998), Climate-convection feedbacks: Some further issues, *Clim. Change*, *39*, 35–38.

Bretherton, C. S., P. N. Blossey, and M. Khairoutdinov (2005), An energy-balance analysis of deep convective self-aggregation above uniform SST, *J. Atmos. Sci.*, *62*, 4273–4292.

Chavas, D. R. (2013), Tropical cyclone size in observations and in radiative-convective equilibrium, PhD thesis, Mass. Inst. of Technol., Cambridge, Mass.

Collins, W. D., et al. (2006), The formulation and atmospheric simulation of the Community Atmosphere Model Version 3 (CAM3), *J. Clim.*, *19*, 2144–2161.

Emanuel, K. A. (1986), An air-sea interaction theory for tropical cyclones. Part I: Steady state maintenance, *J. Atmos. Sci.*, *43*, 585–604.

Grabowski, W. W. (2006), Indirect impact of atmospheric aerosols in idealized simulations of convective–radiative quasi equilibrium. *J. Climate*, *19*, 4664–4682.

Hartmann, D. L., and K. Larson (2002), An important constraint on tropical cloud-climate feedback, *Geophys. Res. Lett.*, *29*(20), 1951, doi:10.1029/2002GL015835.

Held, I. M., and B. J. Soden (2006), Robust responses of the hydrological cycle to global warming, *J. Clim.*, *19*, 5686–5699.

Held, I. M., and M. Zhao (2008), Horizontally homogeneous rotating radiative-convective equilibria at GCM resolution, *J. Atmos. Sci.*, *65*, 2003–2013.

Held, I. M., R. S. Hemler, and V. Ramaswamy (1993), Radiative-convective equilibrium with explicit two-dimensional moist convection, *J. Atmos. Sci.*, *50*, 3909–3927.

Islam, S., R. L. Bras, and K. A. Emanuel (1993), Predictability of mesoscale rainfall in the tropics, *J. Appl. Meteorol.*, *32*, 297–310.

Khairoutdinov, M. F., and K. A. Emanuel (2010), Aggregated convection and the regulation of tropical climate, Preprints, paper presented at the 29th Conference on Hurricanes and Tropical Meteorology, p. 2.69, Am. Meteorol. Soc., Tucson, Ariz.

Khairoutdinov, M. F., and D. A. Randall (2003), Cloud-resolving modeling of the ARM summer 1997 IOP: model formulation, results, uncertainties and sensitivities, *J. Atmos. Sci.*, *60*, 607–625.

Knutson, T. R., et al. (2010) Tropical cyclones and climate change, *Nat. Geosci.*, *3*, 157–163.

Knutson, T. K., R. E. Tuleya, and Y. Kurihara (1998), Simulated increase of hurricane intensities in a CO2-warmed climate, *Science*, *279*, 1018–1021.

Kuang, Z., and D. L. Hartmann (2007), Testing the fixed anvil temperature hypothesis in cloud-resolving model, *J. Clim.*, *20*, 2051–2057.

Lilly, D. K. (1962), On the numerical simulation of buoyant convection, *Tellus*, *14*(2), 148–172.

Muller, C. J., and I. M. Held (2012), Detailed investigation of the self-aggregation of convection in cloud-resolving simulations, *J. Atmos. Sci.*, *69*, 2551–2565.

Nolan, D. S., E. D. Rappin, and K. A. Emanuel (2007), Tropical cyclogenesis sensitivity to environmental parameters in radiative–convective equilibrium, *Q. J. R. Meteorol. Soc.*, *133*, 2085–2107.

Renno´, N. O., K. A. Emanuel, and P. H. Stone (1994), Radiative-convective model with an explicit hydrological cycle, Part I: Formulation and sensitivity to model parameters, *J. Geophys. Res.*, *99*, 14,429–14,441.

Robe, F. R., and K. Emanuel (1996), Dependence of tropical convection on radiative forcing, *J. Atmos. Sci.*, *53*, 3265–3275.

Romps, D. M. (2011), Response of tropical precipitation to global warming, *J. Atmos. Sci.*, *68*, 123–138.

Singh, M. S., and P. A. O'Gorman (2012), Upward shift of the general circulation of the atmosphere in response to global warming, *J. Clim.*, *25*, 8259–8276.

Smolarkiewicz, P. K., and W. W. Grabowski (1990), The multidimensional positive definite advection transport algorithm: Nonoscillatory option, *J. Comput. Phys.*, *86*, 355–375.

Tao, W.-K., J. Simpson, C.-H. Sui, C.-L. Shie, B. Zhou, K. M. Lau, and M. Moncrieff (1999) Equilibrium states simulated by cloud-resolving models, *J. Atmos. Sci.*, *56*, 3128–3139.

Tompkins, A. M., and G. C. Craig (1998), Radiative-convective equilibrium in a three-dimensional cloud ensemble model, *Q. J. R. Meteorol. Soc.*, *124*, 2073–2097.

Wing, A. A., and K. A. Emanuel (2012), Organization of tropical convection: Dependence of self-aggregation on SST in an idealized modeling study, Preprints, paper presented at the 30th Conference on Hurricanes and Tropical Meteorology, p. 12C.4, Am. Meteorol. Soc., Tucson, Ariz.

Xu, K.-M., and D. A. Randall (1999), A sensitivity study of radiative-convective equilibrium in the tropics with a convection-resolving model, *J. Atmos. Sci.*, *56*, 3385–3399.